Combining NOMA and mmWave Technology for Cellular Communication

Syed Ahsan Raza Naqvi and Syed Ali Hassan
School of Electrical Engineering & Computer Science (SEECS)
National University of Sciences & Technology (NUST), Islamabad, Pakistan 44000
Email: {11beesraza, ali.hassan}@seecs.edu.pk

***Abstract*—Non-orthogonal multiple access (NOMA) is a major technique that is expected to lead towards the fifth generation (5G) wireless communication networks, as it involves the sharing of space resources among users in a given scenario. In this paper, we propose an uplink (UL) NOMA setup that utilizes the multiple-input multiple-output (MIMO) infrastructure. As performed in related literature, K clients are placed in 'weak' and 'strong' categories, depending on the channel state information (CSI). The base station (BS) uses successive interference cancellation (SIC) to overcome interference experienced by users forming the weak set from their counterparts in the strong set. The paper goes on to compare the performance of this NOMA system with that of a conventional orthogonal multiple access (OMA) setting, with the scope being extended to include both ultra high frequency (UHF) and millimeter wave (mmWave) networks. The performance evaluation is carried out in terms of, among other metrics, average sum-rate and outage probability.**

***Index Terms*—5G, mmWave, non-orthogonal multiple access, orthogonal multiple access, successive interference cancellation.**

I. Introduction

One of the major motivations behind the introduction of 5G wireless technology in the future is the steady rise in demand for increased data rates across cellular networks [1]. While there are several techniques proposed to leverage high data rates, the requisite levels of sum-capacity may be achieved in two ways, among others. Firstly, it is proposed that a multiple access technique with a high spectral efficiency [2], i.e. NOMA, may be employed. Simply stated, NOMA is a multiplexing scheme that uses the power domain to introduce quasi-orthogonality into the system [3]. Users experiencing better channel gains are paired up with those facing lower channel gains, with the disparity in channel nature being compensated by having greater power allocation for the weak user. Any interference from the strong member in the transmission/reception of the weaker user is removed by the SIC. While the stronger user does indeed encounter interference, its channel state ensures that the intended message is accurately transmitted to the BS.

The second strategy to meet the market demands may be to deploy mmWave-based networks. Since greater bandwidth is also required to provide enhanced data rates, mmWave networks become a natural choice for the upcoming 5G technology. This, along with the prospects of using larger antenna arrays due to small wavelength [4], has meant that research into the use of mmWave in future cellular networks is already underway [5] – [7]. In the past, mmWave technology was not considered to be feasible for wireless communication due to the larger penetration loss. In [8], authors have analyzed mmWave for cellular networks by using highly directional antennas and beamforming to provide coverage in the range of about 150-200 m. It should be stressed that while NOMA introduces interference dependence, using mmWave systems renders the link noise-dependent to a great extent. With the enhanced path loss in mmWave networks, the interference experienced by the users in a NOMA-based network can be significantly reduced, which is the main motivation behind this study. The subsequent sections of this paper aim to compare the performance of networks using UHF and mmWave technologies, considering not only the different bandwidths on offer, but also the distinct path loss models applied to transmissions in each system.

The paper is organized as follows. Section II introduces relevant research work previously conducted in the fields of mmWave communication and NOMA. Section III develops the system model, complete with path loss models and expressions for postcoding matrices and sum capacities for both OMA and NOMA schemes. Section IV compares the cellular network's performance when using OMA and NOMA techniques for both mmWave and UHF technologies. Section V draws conclusions and suggests possible extensions to the tests presented herein.

II. Related Work

In literature, network performance and pairing algorithms in NOMA setups have been investigated for both UL and downlink (DL) transmissions. For instance, [9] puts forth a novel MIMO-NOMA framework for DL and UL transmission by applying the concept of signal alignment. It develops closed-form analytical results to facilitate the performance evaluation of the framework for randomly deployed clients. The effect of various power allocation strategies, e.g. fixed power allocation and cognitive radio inspired power allocation, on the performance of MIMO-NOMA has also investigated. Additionally, [10] proposes a suboptimal algorithm which uses the concept of successive bandwidth division (SBD) in NOMA system, and is primarily aimed at reducing receiver side complexity.

Mmwave-related communication is an emerging field in wireless technologies. In this respect, [5] provides motivation for these new systems by proposing methodology and

978-1-5090-1701-0/16/$31.00 ©2016 IEEE

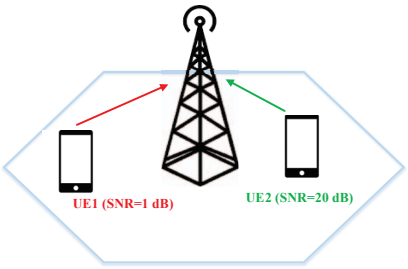

Fig. 1: Uplink NOMA with multiple users.

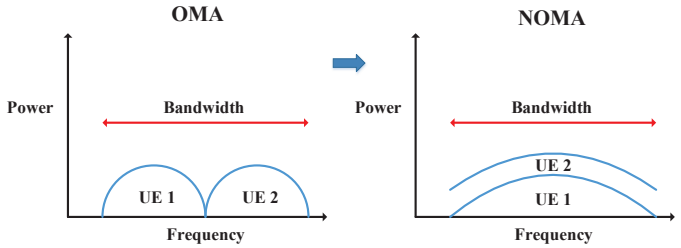

Fig. 2: Simple comparison between OMA and NOMA with K=2.

hardware for measurements. In recent publications, such as [11], the authors have analyzed coverage and rate trends in mmWave cellular networks. Moreover, [4] summarizes the distinguishing features of mmWave networks, apart from introducing models for blockage and beamforming in such systems. Furthermore, [12] implements a cooperative NOMA transmission scheme that considers a scenario in which users in NOMA systems have prior information about the others' messages.

This paper aims to harness both NOMA and mmWave techniques to optimize the usage of a cellular network's resources, as opposed to networks using OMA and UHF technologies. A comparison of outage probabilities and average sum rates has been made with systems using combinations of OMA-UHF, OMA-mmWave, and NOMA-UHF techniques. It has been found that implementing NOMA in mmWave systems helps improve average sum-capacities, in addition to reducing the interference when compared to conventional UHF systems.

III. System Model

This paper considers an UL MIMO system, as depicted in Fig. 1, where the total number of users in the cell is K, and $K \geq 2M$ if M represents the number of antennas employed at the BS. Moreover, each user equipment (UE) has a single antenna. In schemes other than NOMA, the resulting M postcoders can only support M users. Subsequent discussion in this paper will use the term 'set' to represent these M users. The different bandwidths available to clients in the OMA and NOMA schemes are demonstrated in Fig. 2.

The NOMA system presented herein aims to support at least $2M$ randomly deployed users at any given instance. To this end, the clients are categorized into two mutually exclusive sets of 'strong' and 'weak' users, depending on whether the channel gains experienced by them are large (strong set) or small (weak set).

The OMA scheme divides the channel into K sub-bands, which affords each client an orthogonal frequency band for use. However, this division reduces the available bandwidth by a factor of $1/K$, which, in turn, badly affects the user's data rates. In contrast, NOMA accommodates all users, from either set, into a single, large frequency band. While this strategy does indeed improve data rates, it results in interference among the users. Under these circumstances, SIC may be used to mitigate the interference experienced by users of the weak set from those of the strong set. This paper will investigate, among other aspects, the influence of the disparate path loss models of the UHF and mmWave networks on the interference components faced by NOMA clients.

A. Path loss models

Next, we proceed to outlining the path loss models for both UHF and mmWave networks. The path loss model for the mmWave link is similar to that used in [13]. The path loss, $L_{mm}(r)$, in dB, is modeled as,

$$L_{mm}(r) = \rho + 10\alpha \log(r) + \chi_{mm}, \tag{1}$$

whereas the path loss for the UHF link, $L_{UHF}(r)$, in dB, is given by,

$$L_{UHF}(r) = 20 \log(\frac{4\pi}{\lambda_c}) + 10\alpha \log(r) + \chi_{UHF}. \tag{2}$$

In the equations above, r is the distance of the UE from the BS, χ_{mm} is the zero mean log normal random variable for the mmWave link, which models the effects of shadow fading. The fixed path loss in $L_{mm}(r)$ is given by $\rho = 32.4 + 20\log(f_c)$ where f_c is the carrier frequency. The symbol χ_{UHF} represents the shadow fading in UHF links. The path loss exponents for both links are denoted by α.

B. Zero-forcing (ZF) Postcoder for UL NOMA

If the channel matrices, $\mathbf{H}_1$ and $\mathbf{H}_2$, represent the strong and weak sets, respectively, then they may be written as,

$$\mathbf{H}_1 = [\mathbf{h}_{1,1} .... \mathbf{h}_{M,1}], \mathbf{H}_2 = [\mathbf{h}_{1,2} .... \mathbf{h}_{M,2}], \tag{3}$$

where $\mathbf{h}_{n,1}$ and $\mathbf{h}_{m,2}$ denote the $M \times 1$ UL channel vectors of the n^{th} and m^{th} users in each strong and weak set, respectively. We take the UL channel to be the product of path loss and Rayleigh fading with zero mean and unit variance. Thus, in the given scenario, the received signals of the entire group of UL users, $\mathbf{y}$, are given by,

$$\mathbf{y} = (\mathbf{H}_1\mathbf{x}_1 + \mathbf{H}_2\mathbf{x}_2) + \mathbf{n}, \tag{4}$$

where $\mathbf{x}_1 = [\sqrt{\beta_{1,1}}s_{1,1} \dots \sqrt{\beta_{M,1}}s_{M,1}]_T$ and $\mathbf{x}_2 = [\sqrt{\beta_{1,2}}s_{1,2} \dots \sqrt{\beta_{M,2}}s_{M,2}]^{\mathrm{T}}$ are $M \times 1$ transmitted signal vectors of the strong and weak set respectively. $\beta_{n,1}$ and $\beta_{m,2}$ are the power allocation factors for the strong and weak set in that order, s is the message signal, $\mathbf{n}$ is the $M \times 1$ additive white Gaussian noise (AWGN) vector where each value is a normal random variable with zero mean and ${\sigma_n}^2$ variance. In

order to obtain the strong and weak sets, the channel gains are first sorted in descending order, following which this parent set of channel gains of K users is split into two halves; the first half is taken to be the strong set, while the other is the weak set.

A brief comment on SIC is in order. This cancellation scheme is deemed necessary due to the fact that the BS receives the sum of the signals from the two sets, as shown by expression (4). In UL SIC transmissions, the signals originating from the strong set are decoded with interference first. Next, the signals from the weak set are decoded following SIC, that exploits the decoded signals from the strong set. Consequently, the users in the strong set experience interference from other users. As this paper assumes perfect SIC, the decoded user signals in the weak set are free from the inter-set interference due to strong users.

In the past, the ZF scheme has been used in DL multi-antenna systems to maximize capacity, if perfect CSI is assumed at the transmitter. On a similar note, the UL multi-antenna system can also attain maximum capacity with the ZF scheme due to the DL-UL duality. Therefore, the ZF scheme can be used to generate a postcoding matrix. Based on $\mathbf{H}_1$ and $\mathbf{H}_2$ in (1), the corresponding postcoding matrices, $\mathbf{W}_1^u$ and $\mathbf{W}_2^u$ can be obtained by,

$$\mathbf{W}_i = [\mathbf{w}_{1,i}{}^T \mathbf{w}_{2,i}{}^T ... \mathbf{w}_{M,i}{}^T]^T = (\mathbf{H}_i)^*((\mathbf{H}_i)(\mathbf{H}_i)^*)^{-1} \quad (5)$$

where $i \in \{1, 2\}$, and $\mathbf{w}_{n,1}$ and $\mathbf{w}_{m,2}$ are the $1 \times M$ ZF postcoder for the n^{th} and m^{th} users in the strong and weak sets, respectively.

C. Received SINR

We now proceed to determining the signal-to-interference-plus noise ratio (SINR) of members of the strong and weak sets using (4) and (5). As previously stated, signals from the strong set are decoded first. After postcoding for the strong set using $\mathbf{W}_1$, the users' signals in the strong set, $\mathbf{r}_1 = [r_{1,1} \quad r_{2,1} \quad ... \quad r_{M,1}]^T$, are

$$\mathbf{r}_1 = \mathbf{W}_1\mathbf{y} = \mathbf{W}_1\mathbf{H}_1\mathbf{x}_1 + \mathbf{W}_1\mathbf{H}_2\mathbf{x}_2 + \mathbf{W}_1\mathbf{n}. \quad (6)$$

From (6), the signal of the n^{th} user in the strong set is given by,

$$r_{n,1} = \mid \mathbf{h}_{n,1} \mid \sqrt{\beta_{n,1}} s_{n,1} + \sum_{i=1}^{K/2} \mathbf{w}_{n,1}\mathbf{h}_{i,2}\sqrt{\beta_{i,2}} s_{i,2} + \mathbf{w}_{n,1}\mathbf{n}. \quad (7)$$

In (7), the first and second terms represent the desired signals of the strong set and the *inter-set interference* from the weak set, respectively. If it is assumed that the BS is equipped with M antennas and, hence, the number of interferers from the weak set are also M, it may be stated that the strong users are only affected by inter-set interference from the weak users. In this case, each channel vector and the zero-forcing precoding vector satisfies the following condition,

$$\mathbf{w}_{j,1}\mathbf{h}_{n,1} = 0; \forall j \neq n, j \in \{1, 2, ...M\}. \quad (8)$$

Building on this assumption, the SINR for strong users can be written as

$$SINR_{n,1} = \frac{\mid \mathbf{w}_{n,1}\mathbf{h}_{n,1} \mid^2 \beta_{n,1} P_{n,1}}{\sum_{j=1}^{K/2} \mid \mathbf{w}_{n,1}\mathbf{h}_{j,2} \mid^2 \beta_{j,2} P_{j,2} + \sigma_n^2}, \quad (9)$$

where $P_{n,1} = \mid s_{n,1} \mid^2$ is the transmit power.

The SINR for the weaker set is given by,

$$SINR_{n,1} = \frac{\mid \mathbf{w}_{n,2}\mathbf{h}_{n,2} \mid^2 \beta_{n,2} P_{n,2}}{\sigma_n^2}, \quad (10)$$

where $P_{n,2} = \mid s_{n,2} \mid^2$ is the transmit power, and perfect SIC is assumed. By extension, the sum rate, R_i in this case will be,

$$R_i = B \sum_{n=1}^{K/2} \log_2(1 + SINR_{n,i}), i \in \{1, 2\}, \quad (11)$$

wherein B is the bandwidth.

If, however, M and K are such that the resultant matrix is rectangular, then the strong and weak users also encounter interference from other strong and weak users, respectively. Consequently, the strong set is afflicted by a total interference of Ω_1, which can be expanded as,

$$\Omega_1 = \sum_{j=1}^{K/2} \mid \mathbf{w}_{n,1}\mathbf{h}_{j,2} \mid^2 \beta_{j,2} P_{j,2} + \quad (12)$$

$$\sum_{j=1, j\neq n}^{K/2} \mid \mathbf{w}_{n,1}\mathbf{h}_{j,1} \mid^2 \beta_{j,1} P_{j,1}, \quad (13)$$

whereas the interference faced by the weak set in this scenario, denoted by Ω_2, may be written as,

$$\Omega_2 = \sum_{j=1, j\neq n}^{K/2} \mid \mathbf{w}_{n,2}\mathbf{h}_{j,2} \mid^2 \beta_{j,2} P_{j,2}. \quad (14)$$

Finally, the sum capacities of conventional OMA may be written as,

$$R_{i,OMA} = \frac{B}{K} \sum_{n=1}^{K} \log_2(1 + \frac{\mid \mathbf{w}_{n,i}\mathbf{h}_{n,i} \mid^2 P_{n,i}}{\sigma_n^2}). \quad (15)$$

IV. Performance Evaluation

We now present the simulation results of the scenarios under discussion. Unless otherwise mentioned, we assume M to be equal to 2, α to be 3.3 for mmWave systems, as in [13], and 2.5 for UHF-based systems, K to be 8, β_1 to be 0.2 and β_2 to be 0.8, and the transmission power, P, to be 24dBm. The assumed system's cell radius is 1km (where the users are randomly distributed), with UHF networks operating at 3GHz frequency and 10MHz bandwidth. On the other hand, the mmWave network uses a carrier frequency of 94GHz and a bandwidth of 2GHz. It should be noted that mmWave BSs generally use large antenna arrays to compensate for the

path loss experienced by transmissions. However, this paper restricts M's value to 2 to simplify simulations and to draw an adequate comparison with the UHF system. It is worth remembering that recent studies regarding the outdoor channel propagation characteristics for the mmWave network, referred to in literature, consider transmission links established for a distance of up to only 200–300m. The value of the radius is chosen only for a fair comparison between the two modes of transmission under investigation.

Fig. 3 demonstrates the relationship between spectral efficiency and varying values of K. Apart from a general increase in the spectral efficiency for all graphs, caused by an increase in the number of users, rates for OMA are generally lower than those for NOMA due to the factor, K, in (15). NOMA graphs, in contrast, follow a more linear path, with the mmWave-NOMA system providing sum capacities that are approximately 38% higher than those offered by UHF-NOMA systems for K = 40, as interferers using mmWave for communication encounter greater path loss. The greater sum-capacities for NOMA, in spite of inter-set interference, are indicative of the advantage of accommodating a greater number of users within a fixed frequency band, using the same network infrastructure.

Fig. 4 is a plot of average sum-rates versus the cell radius. Both pairs of graphs for UHF and mmWave show some degree of decrease in average sum rate with increase in cell radius. The fall is more pronounced for mmWave networks due to the greater path loss experienced by transmissions in such links. As an indicator, changing the cell radius from 1km to 1.5km reduces the mmWave-NOMA sum-rate by nearly 78%. This decrease in sum-rates with increase in cell radius is so severe that when the radius is set at 2km, the advantage of the superior bandwidth of mmWave technology vanishes completely, as average sum-rates for both UHF-NOMA and UHF-OMA are greater than those of their counterparts using a mmWave setup at this point; thus verifying the fact that mmWave will work optimally for smaller cells as compared to UHF. Graphs for UHF show a gentle decrease in sum-rates owing to lower levels of path loss.

Fig. 5 plots sum-rates against β_2. The plot clearly shows

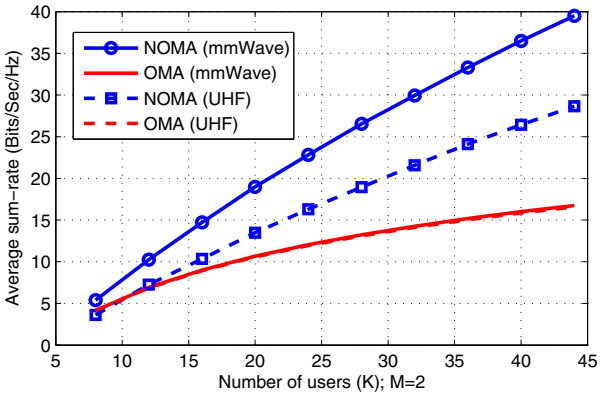

Fig. 3: Spectral efficiency versus number of users.

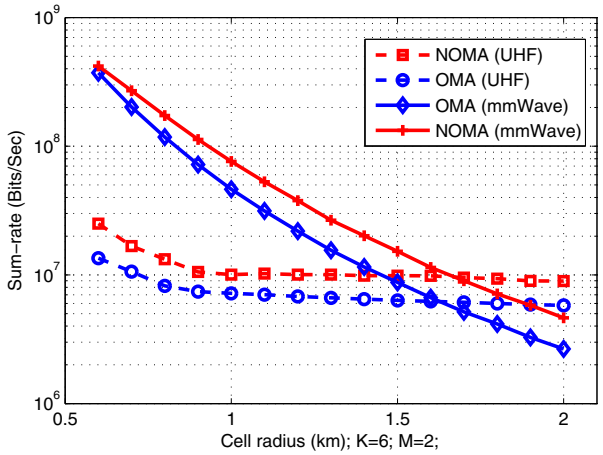

Fig. 4: Average sum-rate versus cell radius.

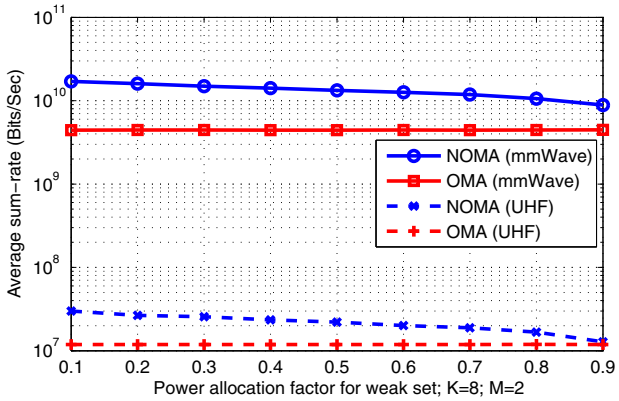

Fig. 5: Average sum-rate versus the power allocation factor, β_2.

the bandwidth advantage afforded by mmWave networks over UHF networks. Graphs for OMA remain invariant, as their expressions are independent of any power allocation factor. Both mmWave-NOMA and UHF-NOMA systems demonstrate a gradual decrease in sum rate with increase in β_2. It may be instructive to note that the gap between NOMA and OMA plots in mmWave scenario is greater than that in UHF scenario, due to the disparate path loss models for the two systems. Smaller values for β_2 result in better rates than larger values do. In fact, at β_2 = 0.9, the average sum rate for NOMA-based UHF networks becomes nearly equivalent to that of the UHF-OMA system, while the sum-rate for mmWave-NOMA continues to be nearly twice that of mmWave-OMA at the given value.

The bar chart in Fig. 6 depicts the variation in Ω_1 with increase in K. Both UHF and mmWave networks exhibit an increase in interference levels with increase in K due to the increase in the sizes of the weak and strong sets. However, the interference components in mmWave cellular networks are smaller than those in UHF networks. In fact, mmWave-NOMA brings about an improvement of 23% in the interference experienced by the strong set for K = 10, as compared to UHF-NOMA. Even when K reaches 90, the mmWave network

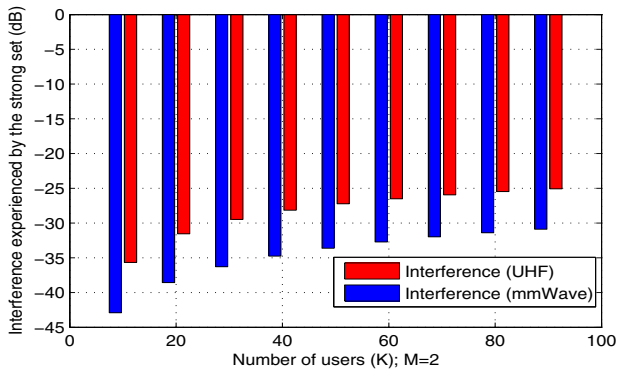

Fig. 6: Interference levels experienced by members of the strong set versus total number of users in the cell.

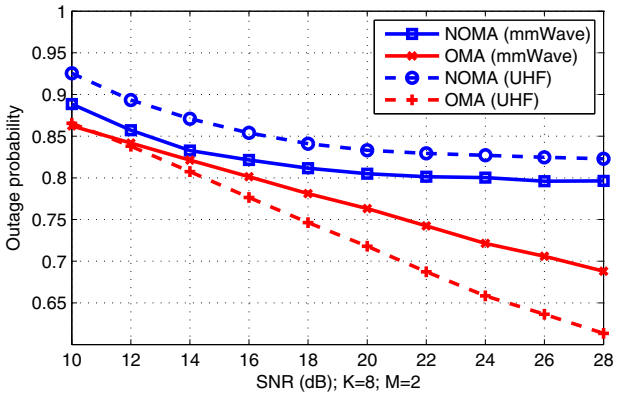

Fig. 7: Outage probability versus operating SNR.

continues to offer approximately 20% less interference. This reduction in interference provides a motivation for marrying mmWave technology with NOMA.

Fig. 7 is the comparison of outage probability against the operating signal-to-noise ratio (SNR). The threshold for outage has been kept at 10dB. The plot shows that NOMA has a greater outage probability in comparison to that for OMA, due to it being interference-limited in nature. However, the mmWave-NOMA performs relatively better in terms of outage as compared to UHF-NOMA, with the former's outage probability being about 3% lower than that of the latter at an SNR of 28dB. In contrast, UHF-OMA consistently has a better outage probability behavior as compared to that of mmWave-OMA. This is due to the available bandwidth for mmWave networks, which is greater than that for UHF networks, and which in turn results in greater noise levels and hence poorer outage performance, as OMA is a noise-limited technique. At an SNR of 28dB, UHF-OMA offers an outage probability that is nearly 14% lower than that of mmWave-OMA. The graphs for both UHF-OMA and mmWave-OMA do not saturate, unlike the graphs for NOMA.

V. Conclusion

This paper has offered a comparison between cellular systems using mmWave and UHF technologies as well as different multiple access techniques, to ascertain the viability of each system to be used as an enabling technology for 5G systems. The results presented herein paint a favorable picture of mmWave-NOMA networks to achieve the enhanced sum capacities required by 5G. The results may be further verified by conducting the tests using set and power-allocation algorithms of varying complexities, as in [14]– [15], to streamline the proposed setup. The simulations may be extended to include massive MIMO technology as well.

References

[1] I. Chih-Lin, C. Rowell, S. Han, Z. Xu, G. Li and Z. Pan, "Toward green and soft: a 5G perspective," *IEEE Commun. Mag.*, vol. 52, no. 2, pp. 66-73, 2014.

[2] S. Chen, K. Peng and H. Jin, "A suboptimal scheme for uplink NOMA in 5G systems," *International Wireless Communication and Mobile Computing (IWCMC) Conference*, pp. 1429-1434, Aug. 2015.

[3] A. Benjebbour, Y. Saito, Y. Kishiyama, A. Li, A. Harada and T. Nakamura, "Concept and practical considerations of non-orthogonal multiple access (NOMA) for future radio access," *International Symposium on Intelligent Signal Processing and Communications Systems (ISPACS)*, pp. 770-774, Nov. 2013.

[4] T. Bai, A. Alkhateeb and R. Heath, "Coverage and capacity of millimeter-wave cellular networks", *IEEE Commun. Mag.*, vol. 52, No.9, pp. 70-77, September 2014.

[5] T. S. Rappaport, S. Sun, R. Mayzus, H. Zhao, Y. Azar, K. Wang, G. N. Wong, J. K. Schulz, M. Samimi and F. Gutierrez, "Millimeter wave mobile communications for 5G cellular: It Will Work!," in *IEEE Access*, vol.1, pp.335-349, 2013.

[6] M. S. Omar, M. A. Anjum, S. A. Hassan, H. Pervaiz and Q. Ni, "Performance analysis of hybrid 5G cellular networks exploiting mmWave capabilities in suburban areas," *IEEE International Conference on Communications (ICC)*, May 2016.

[7] S. A. R. Naqvi, S. A. Hassan and Z. Mulk, "Pilot reuse and sum rate analysis of mmWave and UHF-based massive MIMO systems", *IEEE Vehicular Technology Conference (VTC-Spring)*, May 2016.

[8] T. S. Rappaport, E. Ben-Dor, J. N. Murdock and Yijun Qiao, "38 GHz and 60 GHz angle-dependent propagation for cellular and peer-to-peer wireless communications," *IEEE ICC*, pp. 4568-4573, Jun. 2012.

[9] Z. Ding, R. Schober and H. V. Poor, "A general MIMO framework for NOMA downlink and uplink transmission based on signal alignment," in *CoRR abs/1508.07433*, 2015.

[10] S. Qureshi and S. A. Hassan, "MIMO uplink NOMA with successive bandwidth division," *IEEE Wireless Communications and Networking Conference (WCNC)*, Apr. 2016.

[11] S. Rangan, T. S. Rappaport and E. Erkip, "Millimeter wave cellular wireless networks: Potentials and challenges," in *Proc. IEEE*, vol. 102, no. 3, pp. 366-385, Mar. 2014.

[12] Z. Ding, M. Peng and H. V. Poor, "Cooperative non-orthogonal multiple access in 5G systems," in *IEEE Commun. Lett*, vol. 19, no. 8, pp. 1462-1465, Aug. 2015.

[13] M. N. Kulkarni, S. Singh and J. G. Andrews, "Coverage and rate trends in dense urban mmWave cellular networks," in *IEEE Global Communications Conference (GLOBECOM)*, pp. 3809-3814, Dec. 2014.

[14] Z. Ding, F. Adachi and H. Poor, "The application of MIMO to non-orthogonal multiple access," in *IEEE Trans. Wireless Commun.*, vol. 15, no. 1, pp. 537-552, Jan. 2016.

[15] Z. Ding, P. Fan and V. Poor, "Impact of user pairing on 5G non-orthogonal multiple access downlink transmissions," in *IEEE Trans. Veh. Technol.*, Sep. 2015.